Supplementary Information - Figures

Endoplasmic Reticulum Ca^{2+} Increases Enhance Mutant Glucocerebrosidase Proteostasis

Derrick Sek Tong Ong,[1] Ting-Wei Mu,[1] Amy E. Palmer,[2] and Jeffery W. Kelly[1,*]

[1]Departments of Chemistry and Molecular and Experimental Medicine, The Skaggs Institute for Chemical Biology, The Scripps Research Institute, La Jolla, CA 92037 and [2]Department of Chemistry and Biochemistry, University of Colorado, Boulder, CO 80309

[*]To whom correspondence should be addressed.

Telephone: 858-784-9605

Fax: 858-784-9610

E-mail: jkelly@scripps.edu

Supplementary Figures

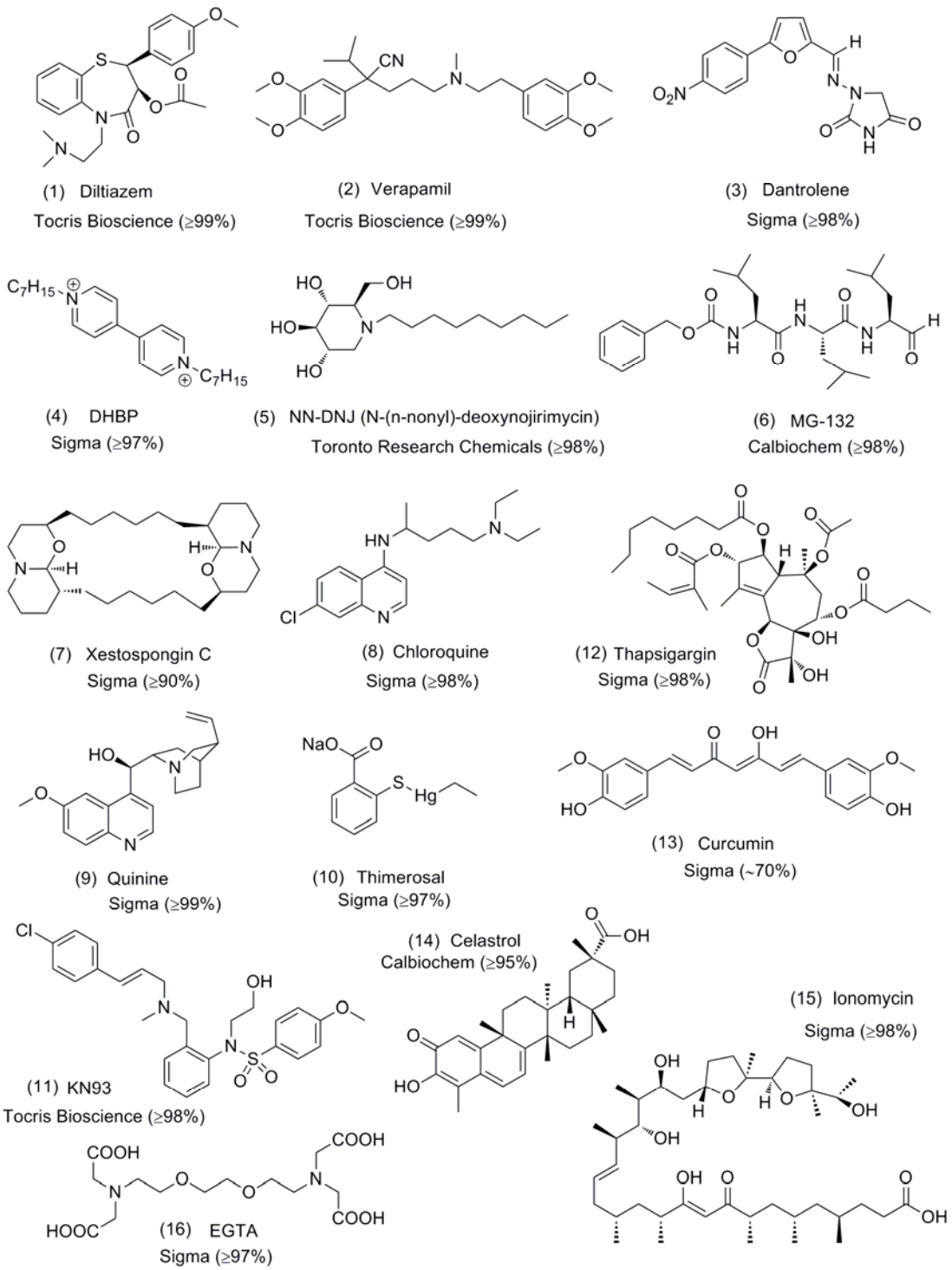

Supplementary Figure 1. Chemical structure of compounds utilized or discussed in the manuscript. The source and purity are also included.

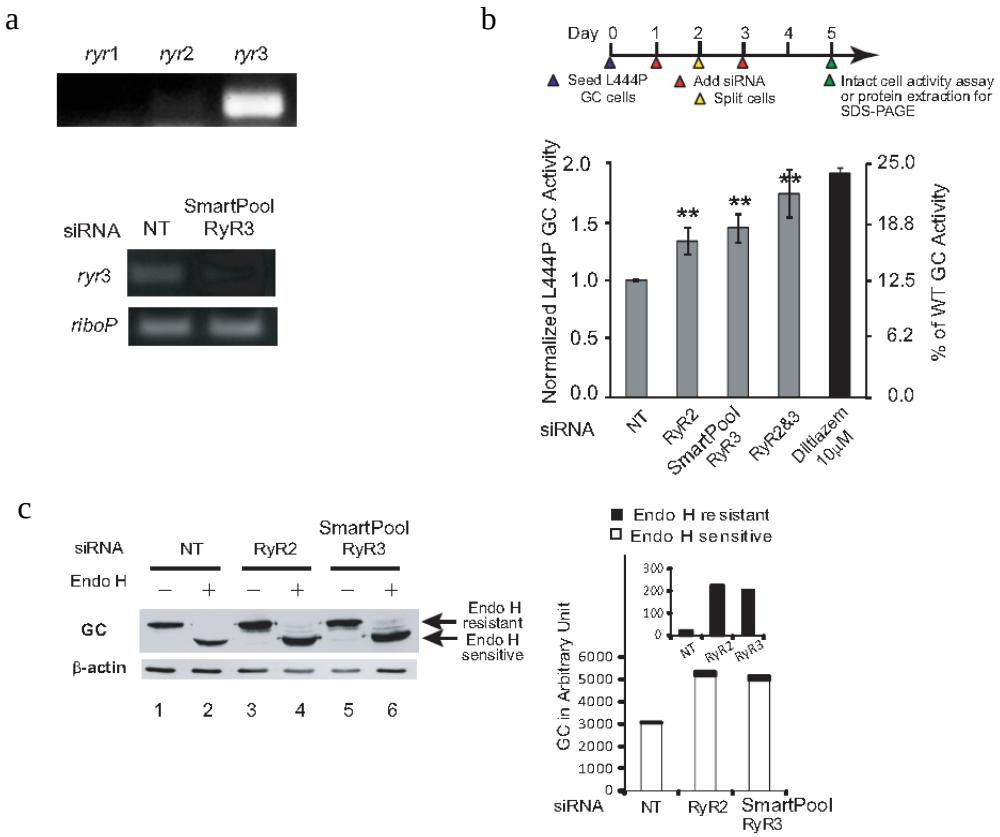

Supplementary Figure 2. The RyRs influence L444P GC proteostasis. Relative RyR isoform expression levels in the L444P fibroblasts (top) and the significant reduction in RyR3 mRNA levels when the SmartPool RyR3 siRNA was used for transfection (bottom) (**a)**. The large ribosomal protein, RiboP, serves as a housekeeping gene control. The siRNA knockdown of RyR2 and RyR3 (using SmartPool siRNA) alone, or in combination, enhances the enzymatic activity (**b**), folding and trafficking (**c**) of the L444P GC in patient-derived fibroblasts revealed by Endo H resistance. The data in (**b**) is reported as mean ± SEM.

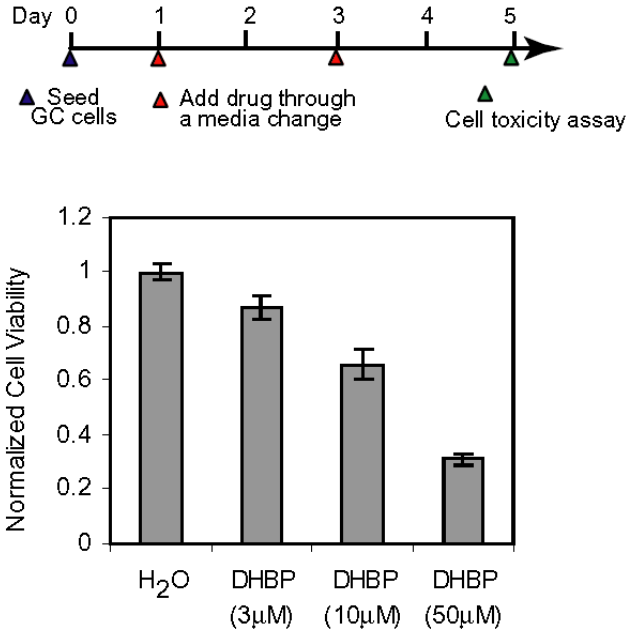

Supplementary Figure 3. DHBP **4** causes cell toxicity to L444P GC patient-derived fibroblasts. Incubation of L444P fibroblasts with DHBP **4** at 3, 10 and 50 μM for 4 d results in a concentration-dependent decrease in cell viability, as determined using the resazurin assay. The data are reported as mean ± SEM.

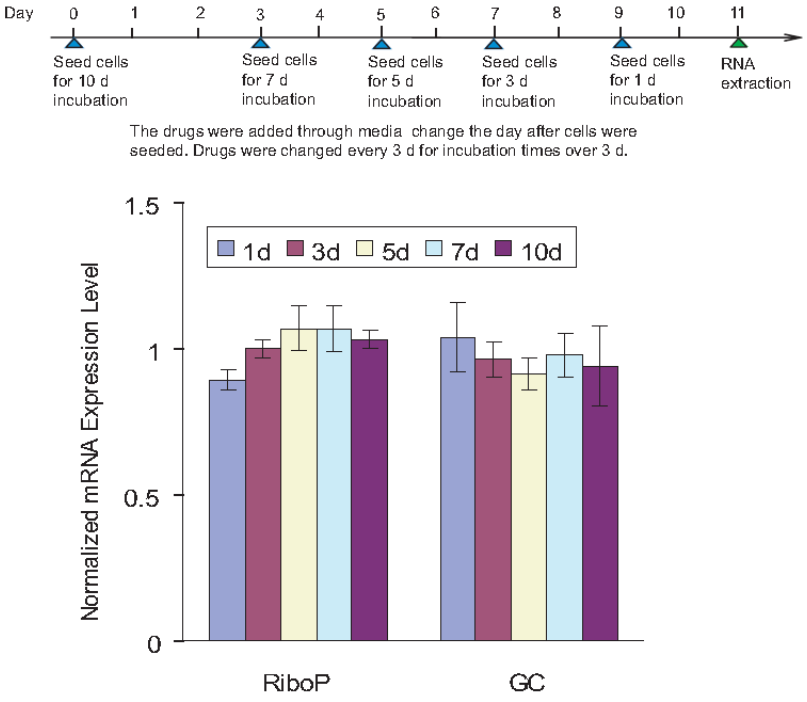

Supplementary Figure 4. Dantrolene **3** does not partially restore L444P GC proteostasis by upregulating L444P GC gene expression. L444P fibroblasts were treated with 10 μM dantrolene **3** for the indicated amount of time before being subjected to cell lysis for qRT-PCR analysis. The large ribosomal protein, RiboP, serves as a housekeeping gene control.

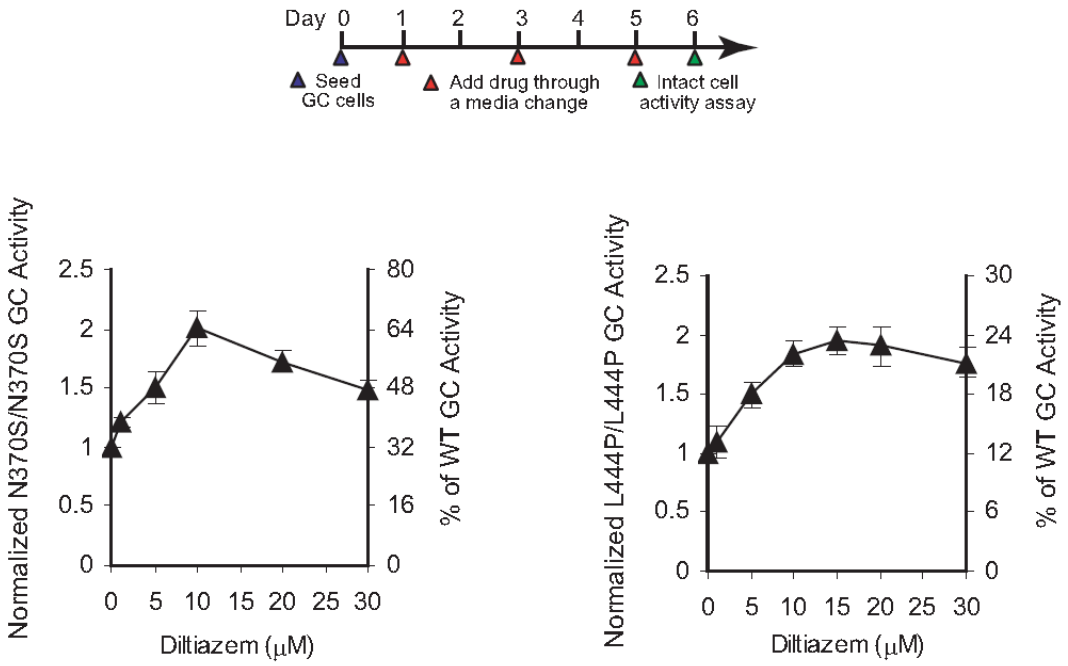

Supplementary Figure 5. Diltiazem **1** increases the N370S and L444P GC enzyme activity significantly in patient-derived fibroblasts, as reported previously[1]. L444P fibroblasts were treated with diltiazem **1** for 5 d before the intact cell activity assay was performed. The data are reported as mean ± SEM.

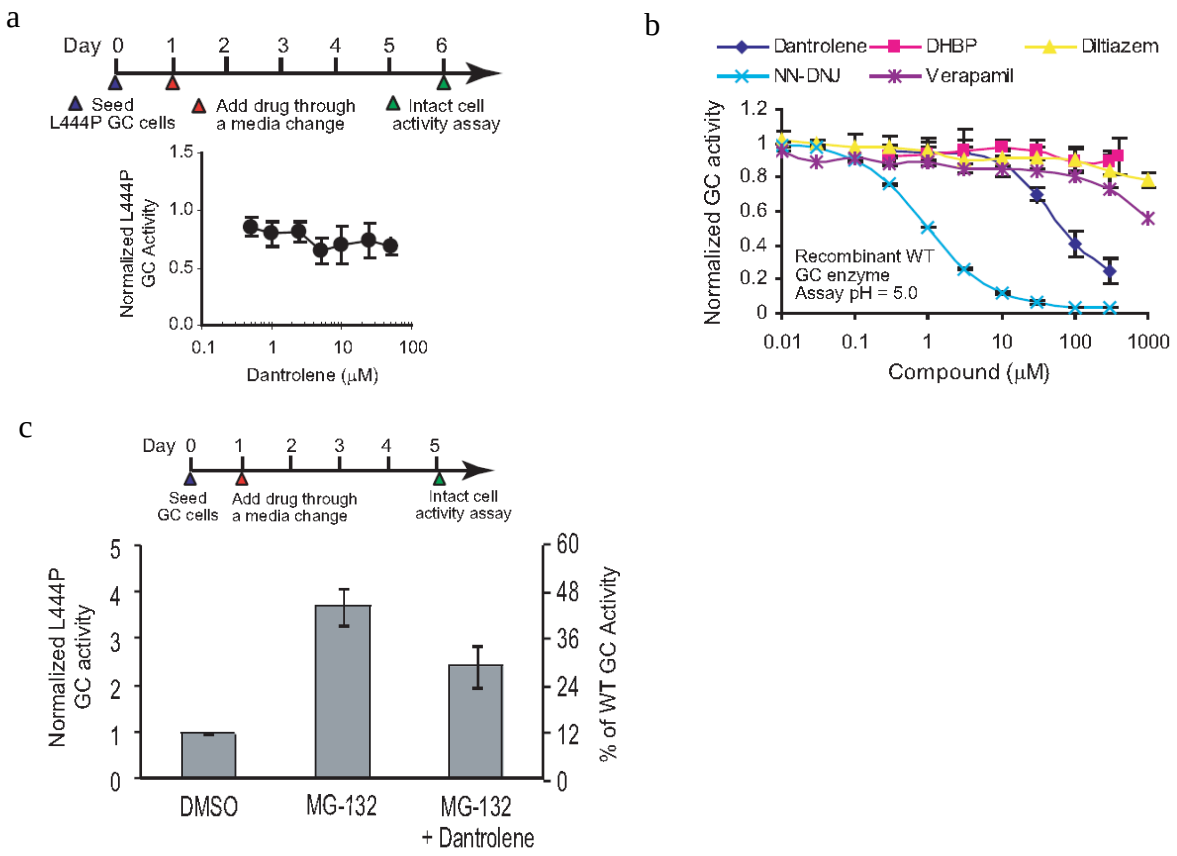

Supplementary Figure 6. Dantrolene **3** partially inhibits the activity of the hypersensitive L444P GC. Dantrolene **3** decreases L444P GC enzyme activity (intact cell assay), due to inhibition of the hypersensitive L444P GC enzyme (**a**). Dantrolene **3** weakly inhibits the WT GC enzyme *in vitro* (**b**). DHBP **4**, diltiazem **1** and verapamil **2** are unlikely to influence GC proteostasis by pharmacologic chaperoning as they do not inhibit WT GC. Data for diltiazem **1** and N-(*n*-nonyl)deoxynojirimycin (NN-DNJ) **5**, previously reported[12], are included for comparison. Dantrolene **3** diminishes the increase in L444P GC activity that is afforded by the MG-132 **6** treatment of patient-derived fibroblasts, normalized to the DMSO vehicle control (**c**). L444P fibroblasts were treated with 0.25 μM MG-132 **6** in the absence or presence of 10 μM dantrolene **3** for 4 d before the intact cell GC activity assay was performed. The data are reported as mean ± SEM.

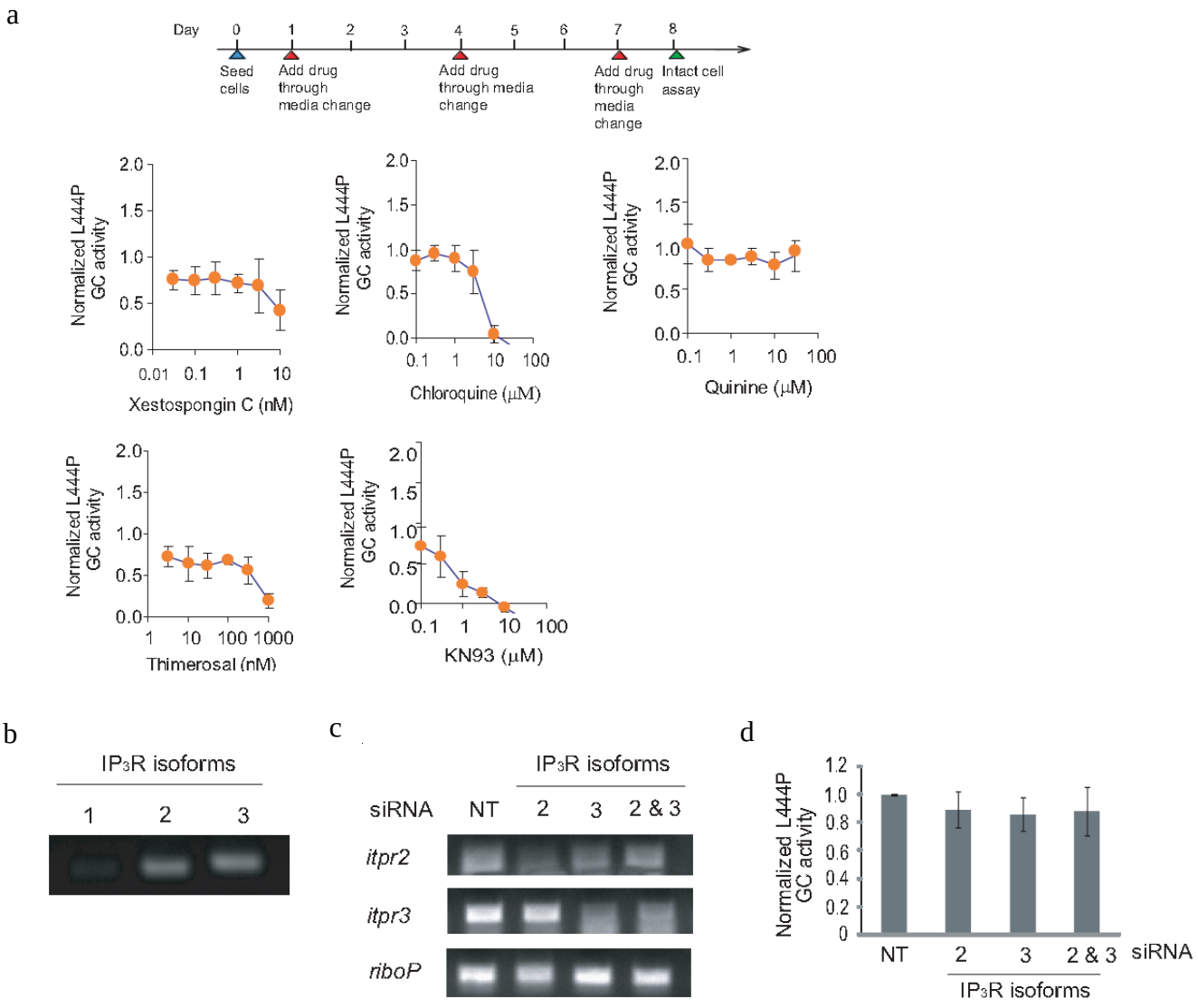

Supplementary Figure 7. Antagonists or siRNAs of the IP_3 receptor do not increase L444P GC enzyme activity in patient-derived fibroblasts. L444P fibroblasts were treated with Xestospongin C (XeC) **7**, chloroquine **8**, quinine **9**, thimerosal **10**, or KN93 **11** (antagonists of the IP_3 receptor) for 7 d before the intact cell activity assay was performed (**a**). The drug treated-L444P GC activity data was normalized to the DMSO vehicle control. Relative IP_3R isoform transcript levels in the L444P fibroblasts (**b**). The IP_3R isoforms 2 and 3 are efficiently knocked down in the L444P fibroblasts using the respective siRNAs (**c**). siRNA knockdown of the IP_3R isoforms 2 and 3 did not change the L444P GC enzyme activity in

homozygous patient-derived fibroblasts (**d**). L444P GC enzyme activity was determined using the intact cell assay, normalized to the non-targeting siRNA control. The data in (**a**) and (**d**) are reported as mean ± SD.

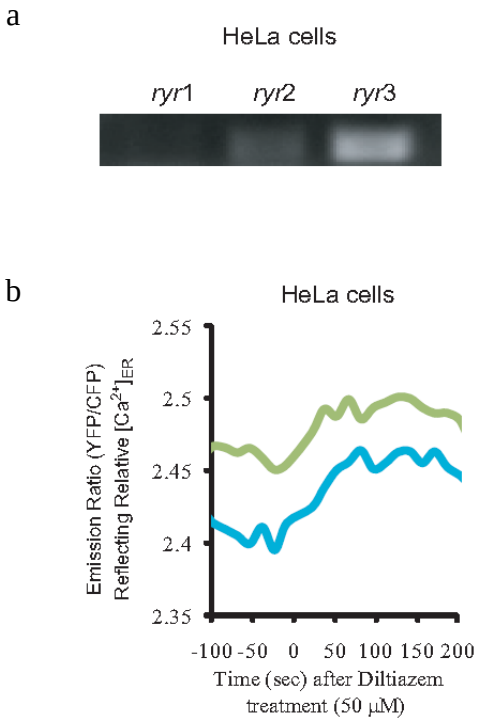

Supplementary Figure 8. Diltiazem **1** treatment (50 μM) acutely increases $[Ca^{2+}]_{ER}$ levels in the HeLa cells that exhibit similar RyR isoforms expression pattern to the L444P fibroblasts. The RyR isoform 3 is most abundantly expressed in the HeLa cells (**a**). Treatment of HeLa cells with 50 μM diltiazem **1** increases $[Ca^{2+}]_{ER}$ over a 200 s time course (**b**). HeLa cells in 35-mm dishes were transfected with 1 μg of D1-ER cameleon-encoding plasmid. After 2-3 days, cells were imaged in 50 μM diltiazem **1** (each trace represents an individual cell). Similar effects were seen from 3 separate experiments.

a

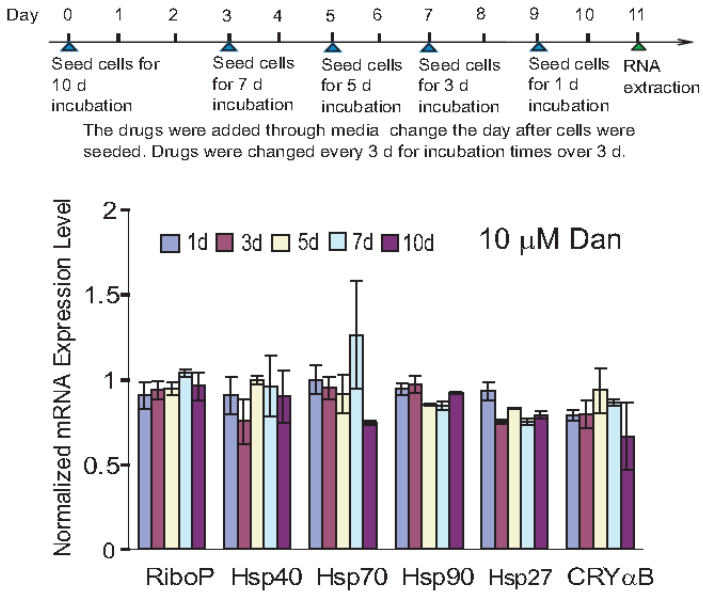

b

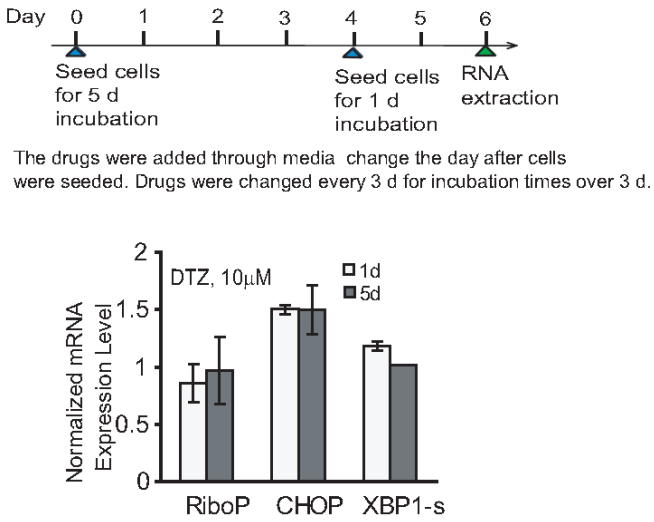

Supplementary Figure 9. Dantrolene **3** and diltiazem **1**[1] do not activate the HSR and UPR. Dantrolene **3** (10 μM) does not activate the HSR based on transcriptional analysis of representative chaperones (**a**). Diltiazem **1** (10 μM) does not activate the UPR based on transcriptional analysis of CHOP (the reporter of the PERK arm) and spliced XBP-1 (the reporter of the IRE1 arm) (**b**).

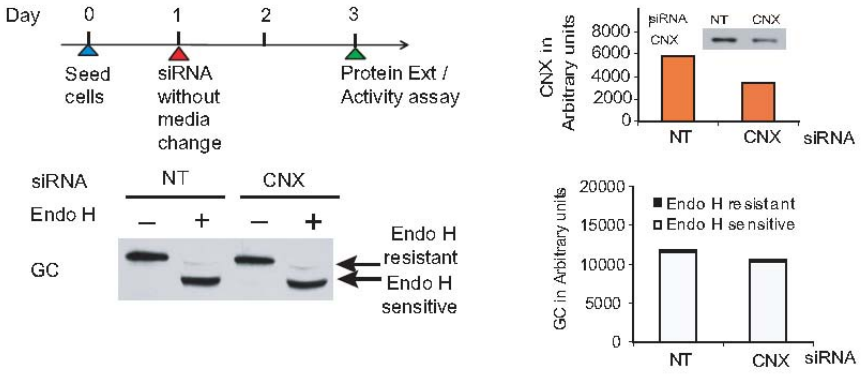

Supplementary Figure 10. siRNA knockdown of calnexin did not significantly change the endo H resistant L444P GC protein band intensity when compared with the non-targeting siRNA control. The levels of calnexin after the siRNA treatment and the resulting GC band intensities are shown on the top and bottom right, respectively.

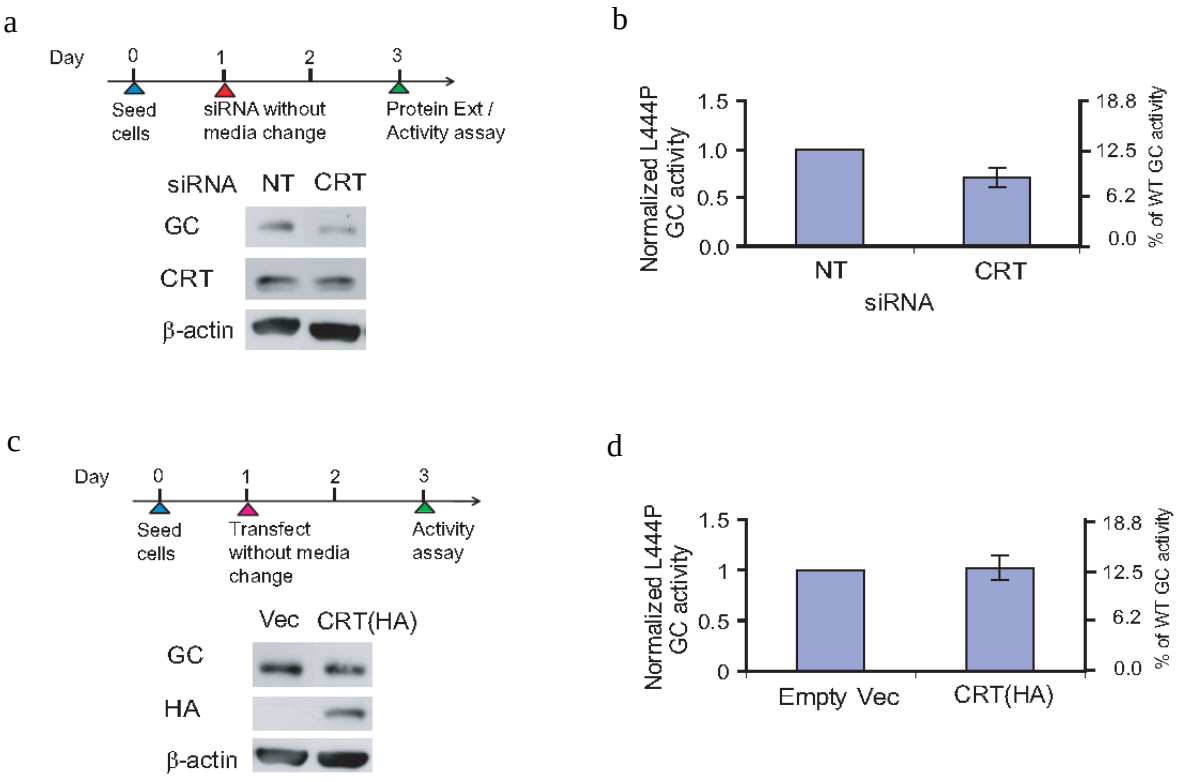

Supplementary Figure 11. Calreticulin's (CRT) influence on L444P GC proteostasis. siRNA knockdown of calreticulin led to a significant decrease in the L444P GC protein level (**a**) and enzyme activity (**b**) in patient-derived fibroblasts. However, the transient overexpression of calreticulin in L444P fibroblasts did not significantly increase total L444P GC levels (**c**) or enzyme activity (**d**). L444P GC enzyme activity was determined using the intact cell assay. The data in (**b**) and (**d**) are normalized to the non-targeting siRNA and empty vector controls, respectively, and reported as mean ± SD.

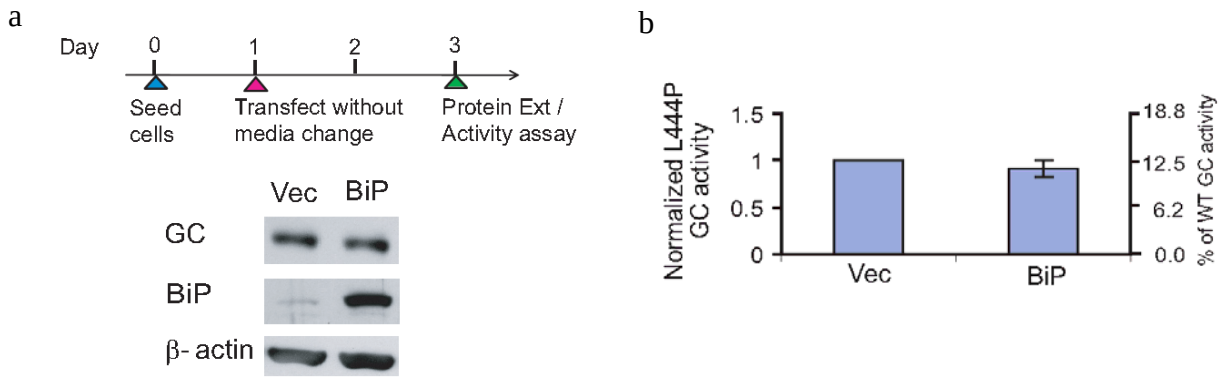

Supplementary Figure 12. Overexpression of BiP does not significantly influence L444P GC proteostasis. The transient overexpression of BiP in the L444P fibroblasts did not significantly increase total L444P GC protein levels (**a**) or enzyme activity **(b)**. L444P GC enzyme activity was determined using the intact cell assay, normalized to the empty vector control. The data in (**b**) are reported as mean ± SD.

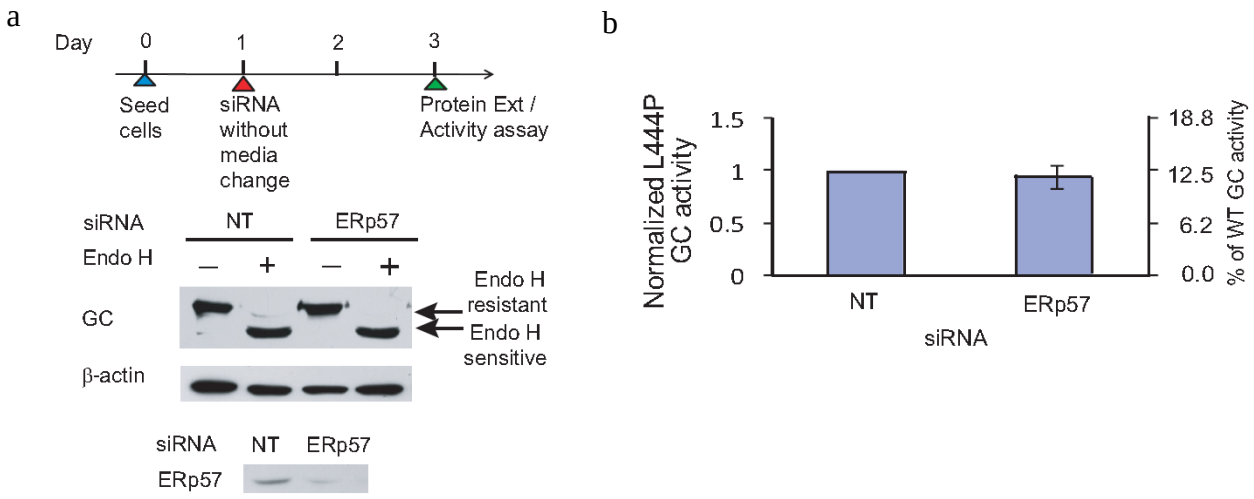

Supplementary Figure 13. RNAi of ERp57 does not significantly influence L444P GC proteostasis. siRNA knockdown of ERp57 did not change total L444P GC protein levels (**a**) or enzyme activity (**b**) in homozygous patient-derived fibroblasts. L444P GC enzyme activity was determined using the intact cell assay, normalized to the non-targeting siRNA control. The data in (**b**) are reported as mean ± SD.

Table S1. Primer sequences used in quantitative RT-PCR

Gene	GenBank Accession Code	Forward Primer	Reverse Primer
GC	M16328	5'-CTC CAT CCG CAC CTA CAC C-3'	5'-ATC AGG GGT ATC TTG AGC TTG G-3'
RiboP	NM_001004	5'-CGT CGC CTC CTA CCT GCT-3'	5'-CCA TTC AGC TCA CTG ATA ACC TTG-3'
Hsp40	NM_006145	5'-CGC CGA GGA GAA GTT C-3'	5'-CAT CAA TGT CCA TGC CTT-3'
Hsp70	NM_005345	5'-GGA GGC GGA GAA GTA CA-3'	5'-GCT GAT GAT GGG GTT ACA-3'
Hsp90	NM_005348	5'-GAT AAA CCC TGA CCA TTC C-3'	5'-AAG ACA GGA GCG CAG TTT CAT AAA-3'
Hsp27	X54079	5'-AAG TTT CCT CCT CCC TGT CC-3'	5'-CGG GCT AAG GCT TTA CTT GG-3'
CRYAB	NM_001885	5'-CAC CCA GCT GGT TTG ACA CT-3'	5'-TGA CAG AGA ACC TGT CCT TCT-3'
CHOP	NM_004083	5'-ACC AAG GGA GAA CCA GGA AAC G-3'	5'-TCA CCA TTC GGT CAA TCA GAG C-3'
Xbp1-s	NM_005080	5'-CCG CAG CAG GTG CAG G-3'	5'-GAG TCA ATA CCG CCA GAA TCC A-3'
RyR1	NM_000540	5'-CCT GCG CCG CTC AGC TG-3'	5'-CCT TCT TGG CCT TGA ATA AGA AGC C-3'
RyR2	NM_001035	5'-CTG GAG CCA GTG TCA TCC ACC-3'	5'-GTG ATG CAA CTG ATG AAA TCC CTG AAT G-3'
RyR3	NM_001036	5'-GCG ACA ATT CTG GAC AGT CAA CTT CC-3'	5'-CCC ACA GTG TAT GTC CAT TAG GC-3'
ITPR1	NM_001099952	5'-GCG GAG GGA TCG ACA AAT GG-3'	5'-TTT TGG GCA GAG TAG CGG TTC-3'
ITPR2	NM_002223	5'-AAG GAG GGG ACG TTG TTA GAT-3'	5'-ACC ACC TCT ATT TCC CAG AGT G-3'
ITPR3	NM_002224	5'-TGA CGT GTG ACG AGT ACA AGG-3'	5'-TGA AGC GGT ACAA GCC ATT CC-3'

Supplementary Information – Methods

Endoplasmic Reticulum Ca^{2+} Increases Enhance Mutant Glucocerebrosidase Proteostasis

Derrick Sek Tong Ong,[1] Ting-Wei Mu,[1] Amy E. Palmer,[2] and Jeffery W. Kelly[1,*]

[1]Departments of Chemistry and Molecular and Experimental Medicine, The Skaggs Institute for Chemical Biology, The Scripps Research Institute, La Jolla, CA 92037 and [2]Department of Chemistry and Biochemistry, University of Colorado, Boulder, CO 80309

[*]To whom correspondence should be addressed.

Telephone: 858-784-9605

Fax: 858-784-9610

E-mail: jkelly@scripps.edu

Supplementary methods

Reagents. Diltiazem hydrochloride was from Tocris Bioscience (Ellisville, MO). Dantrolene sodium, DHBP dibromide, 4-methylumbelliferyl β-D-glucoside (MUG), EGTA, and EDTA were from Sigma (St. Louis, MO). Conduritol B epoxide (CBE) and N-(n-nonyl)-deoxynojirimycin were from Toronto Research Chemicals (Downsview, ON, Canada). Celastrol and MG-132 were from Calbiochem (San Diego, CA). All the other tested small molecules were either from Tocris Bioscience or from Sigma. Cell culture media were obtained from Gibco (Grand Island, NY). Human injection quality recombinant WT GC protein (trade name Cerezyme) was obtained from Genzyme (Cambridge, MA).

Cell cultures. Apparently normal fibroblasts (GM00498) and homozygous Gaucher fibroblasts containing the L444P GC (c.1448T>C) mutation (GM08760) were obtained from the Coriell Cell Repositories (Camden, NJ). Primary skin fibroblast culture was established from Gaucher patients homozygous for the N370S GC (c.1226A>G) mutation. Fibroblasts were grown in minimal essential medium with Earle's salts supplemented with 10 % heat-inactivated fetal bovine serum and 1 % glutamine Pen-Strep at 37 °C in 5 % CO_2. Cell medium was replaced every 3 or 4 d. Monolayers were passaged upon reaching confluency with TrypLE Express.

Enzyme activity assays. The intact cell GC activity assay was performed as previously described[2]. Briefly, approximately 10^4 cells were plated in each well of a 96-well plate (100 μl per well) overnight to allow cell attachment. Medium was replaced with fresh medium containing small molecules as indicated in each figure and plates were incubated at 37 °C. Cell viability after drug treatment was measured using the resazurin assay. The medium was then removed and monolayers washed with PBS. The assay reaction was started by the addition of 50 μl of 2.5 mM MUG in 0.2 M acetate buffer (pH 4.0) to each well. Plates were incubated at 37 °C for 1-7 h and the reaction was stopped by the addition of 150 μl of 0.2 M glycine buffer (pH 10.8) to each well. Liberated 4-methylumbelliferone was measured (excitation 365 nm,

emission 445 nm) using a SpectraMax Gemini plate reader (Molecular Device, Sunnyvale, CA). Control experiments to evaluate the extent of unspecific non-lysosomal GC activity were performed by adding CBE to the assay reaction. GC activities measured were normalized to the corresponding cell number for each sample. This assay is good at predicting what would likely happen in a patient.

The lysed cell GC activity was assayed as previously described[2]. Briefly, intact cells were harvested and the pellet was lysed in complete lysis-M buffer containing complete protease inhibitor cocktails (Roche #10799050001). Total cell protein was measured using the Micro BCA assay reagent (Pierce, Rockford, IL, #23235). 40 μg of total cell protein was assayed for GC activity in 100 μl of 0.1 M acetate buffer (pH 5.0) containing 3 mM MUG in the presence of 0.15 % Triton X-100 (v/v, Fisher) and 0.15 % taurodeoxycholate (w/v, Calbiochem). CBE was used as a control to evaluate the extent of non-lysosomal GC activity. After incubation at 37 °C for 1 to 7 h, the reaction was terminated with 200 μl of 0.2 M glycine buffer (pH 10.8), and the fluorescence was recorded (excitation 365 nm, emission 445 nm). This assay is accompanied by dilution and therefore it gives a more accurate reflection of an increase in folding, trafficking and function accomplished by a compound that can inhibit GC enzyme activity, however the intact cell assay is better at predicting what will likely happen in a patient.

The GC activity assay for recombinant WT GC enzymes has been previously described[3]. 25 ng of recombinant WT GC protein was assayed for GC activity in 50 μl of 0.1 M acetate buffer (pH 5.0) containing 3 mM MUG in the presence of 0.15 % Triton X-100 (v/v, Fisher) and 0.15 % taurodeoxycholate (w/v, Calbiochem). After the addition of tested compounds, the reaction was incubated at 37 °C for 20 min, terminated with 75 μl of 0.2 M glycine buffer (pH 10.8), and the fluorescence was recorded (excitation 365 nm, emission 445 nm).

Western blot analysis. Cells were lysed with complete lysis-M buffer containing complete protease inhibitor cocktail (Roche, Nutley, NJ). Total cell protein was determined with Micro BCA assay reagent

(Pierce, Rockford, IL) and each sample was diluted to the same protein concentration. Company specifications were followed for protein treatment with Endo H (New England Biolabs, Ipswich, MA). Aliquots of cell lysates were separated in a 10 % SDS-PAGE gel and Western blot analysis was performed using appropriate antibodies. Rabbit anti-Hsp70 and anti-calnexin, as well as mouse anti-Hsp90 and anti-calreticulin were from Stressgen (Victoria, BC, Canada). Rabbit polyclonal anti-GC (G4171) and mouse monoclonal anti-β-actin were from Sigma (St. Louis, MO). Rabbit anti-BiP, anti-GRP94, and anti-Erp57 were from Santa Cruz Biotechnology. Rabbit anti-SERCA2 was from Novus Biologicals (Littleton, CO). Secondary goat anti-rabbit and goat anti-mouse HRP-conjugated antibodies were from Pierce. Blots were visualized using SuperSignal West Femto Maximum Sensitivity or West Pico Substrate (Pierce). The Western blot bands of the endo H treated samples were quantified using NIH Image J software (http://rsb.info.nih.gov/ij/).

ER Ca^{2+} Imaging. Genetically encoded Ca^{2+} indicator, D1-ER cameleon was used to measure ER Ca^{2+} levels, as previously described[4]. Briefly, L444P fibroblasts and HeLa cells were plated on 35-mm glass-bottomed dishes and transfected the next day with 1 μg of D1-ER cameleon using Fugene 6. The cells were washed with Hanks balanced salt solution containing 20 mM HEPES (pH 7.4) (HHBSS) 2-3 days after transfection and imaged using a Zeiss Axiovert 200M microscope with a Cascade 512B cooled charge-coupled device camera, controlled by METAFLUOR 6.1 software. Emission ratio imaging of the ER cameleon was accomplished using a 430/24 excitation filter, 450-nm dichroic mirror, and two emission filters (470/24 for CFP and 535/20 for YFP) controlled by a Lambda 10-3 filter changer. For the acute drug treatment experiment, D1-ER cameleon transfected cells were washed with HHBSS, and drugs were added to 35-mm glass-bottomed dishes and the emission ratio was monitored over a time course of 10 min. For the chronic drug treatment experiment, cells in 35-mm dishes were transfected with Fugene 6 and 1 μg of D1-ER cameleon. The next day, drugs were added, and the cells were incubated for another 2

d. On the day of the imaging experiment, cells were washed with HHBSS to remove drugs and ER Ca^{2+} was imaged under the microscope to determine the steady state $[Ca^{2+}]_{ER}$. To obtain the depleted ER Ca^{2+} state, cells were first treated with 5 μM thapsigargin; once $[Ca^{2+}]_{ER}$ reached a plateau, the cells were further treated with 7.5 mM EGTA and 5 μM ionomycin to completely deplete $[Ca^{2+}]_{ER}$ and obtain the minimum YFP/CFP ratio.The background corrected fluorescence ratio of (YFP/CFP) upon excitation of CFP is a measure of relative ER Ca^{2+} levels. An increase in the resting ratio without an increase in the minimum ratio is indicative of an increase in resting Ca^{2+} levels. Three separate experiments were performed for one drug treatment condition.

Quantitative RT-PCR. The relative expression levels of target genes were analyzed using quantitative RT-PCR as described[1,5]. The cells were incubated with drugs at 37 °C for the indicated amount of time before total RNA was extracted from the cells using RNeasy Mini Kit (Qiagen #74104). cDNA was synthesized from 500 ng of total RNA using QuantiTect Reverse Transcription Kit (Qiagen #205311). Quantitative PCR reactions (45 cycles of 15 s at 94°C, 30 s at 57°C, and 30 s at 72°C) were performed using cDNA, QuantiTect SYBR Green PCR Kit (Qiagen #204143) and corresponding primers in the ABI PRISM 7900 system (Applied Biosystems) and analyzed using SDS2.1 software (Applied Biosystems). The forward and reverse primers for the genes analyzed are listed in Table S1. Threshold cycle (C_T) was extracted from the PCR amplification plot and the ΔC_T value defined as: $\Delta C_T = C_T$ (target gene) - C_T (housekeeping gene). The relative mRNA expression level of a target gene of drug-treated cells was normalized to that of untreated cells: Relative mRNA expression level = 2 exp [- (ΔC_T (treated cells) - ΔC_T (untreated cells))]. Each data point was evaluated in triplicate, and measured three times.

Cell toxicity assay. One thousand L444P fibroblasts were plated in a 96-well plate (Costar) and incubated overnight. Drugs were added to the 100 μl cell culture media and the plates were incubated at 37 °C until the cell toxicity assay was performed. Resazurin (10 μl of 10 mg/ml in PBS) was added to each well and

the plates were incubated for 2 h at 37 °C. The fluorescence signal, which is proportional to cell metabolism/viability, was monitored on a fluorescence plate reader (Molecular Devices) using an excitation wavelength of 530 nm and emission wavelength of 590 nm. Data from at least eight replicates are shown and are reported as mean ± SEM.

Supplementary References

1. Mu, T.W., Fowler, D.M. & Kelly, J.W. Partial restoration of mutant enzyme homeostasis in three distinct lysosomal storage disease cell lines by altering calcium homeostasis. *PloS. Biol.* **6**, 253-265 (2008).
2. Sawkar, A.R. et al. Chemical chaperones increase the cellular activity of N370S beta-glucosidase: a therapeutic strategy for Gaucher disease. *Proc. Natl. Acad. Sci. U S A* **99**, 15428-33 (2002).
3. Sawkar, A.R. et al. Chemical chaperones and permissive temperatures alter the cellular localization of Gaucher disease associated glucocerebrosidase variants. *ACS Chem. Biol.* **1**, 235-251 (2006).
4. Palmer, A.E., Jin, C., Reed, J.C. & Tsien, R.Y. Bcl-2-mediated alterations in endoplasmic reticulum Ca^{2+} analyzed with an improved genetically encoded fluorescent sensor. *Proc. Natl. Acad. Sci. USA* **101**, 17404-17409 (2004).
5. Mu, T.W. et al. Chemical and biological approaches synergize to ameliorate protein-folding diseases. *Cell* **134**, 769-781 (2008).

Supplementary Information – Original Images

Endoplasmic Reticulum Ca^{2+} Increases Enhance Mutant Glucocerebrosidase Proteostasis

Derrick Sek Tong Ong,[1] Ting-Wei Mu,[1] Amy E. Palmer,[2] and Jeffery W. Kelly[1,*]

[1]Departments of Chemistry and Molecular and Experimental Medicine, The Skaggs Institute for Chemical Biology, The Scripps Research Institute, La Jolla, CA 92037 and [2]Department of Chemistry and Biochemistry, University of Colorado, Boulder, CO 80309

[*]To whom correspondence should be addressed.

Telephone: 858-784-9605

Fax: 858-784-9610

E-mail: jkelly@scripps.edu

Figure 1

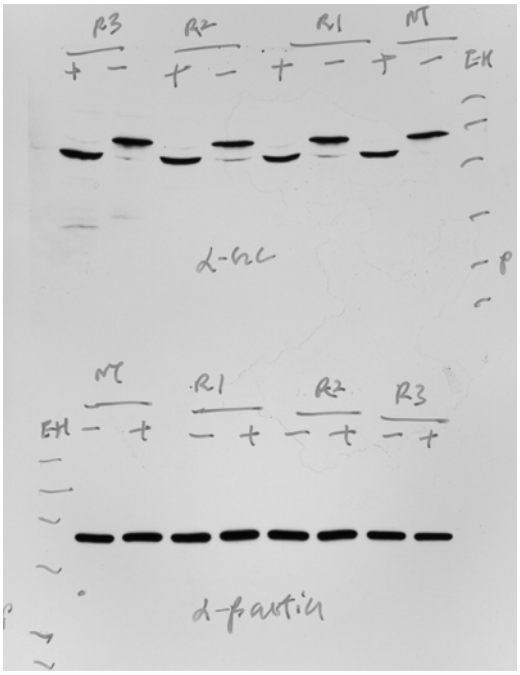
R3
R2
R1
NT
EH
α-hC
P
NT
R1
R2
R3
EH
α-partin

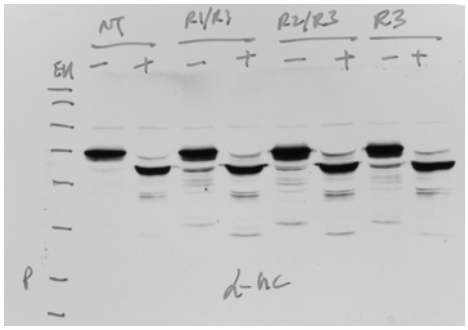
NT
R1/R3
R2/R3
R3
EH
P
α-hC

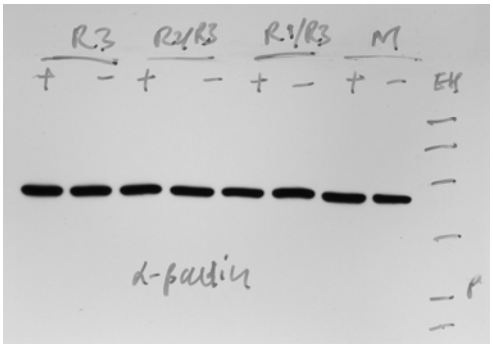
R3
R2/R3
R1/R3
NT
EH
α-partin
P

Figure 2

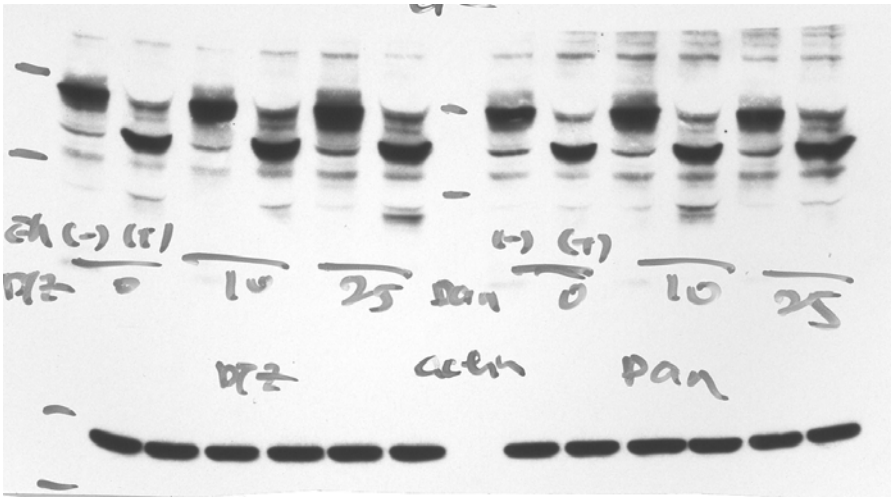

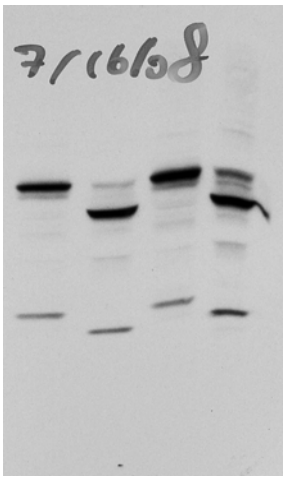

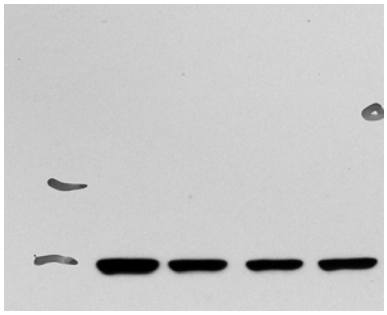

Figure 3

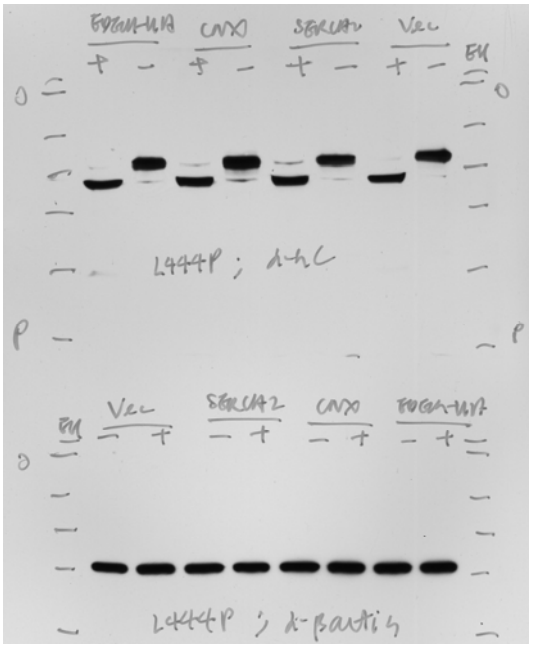

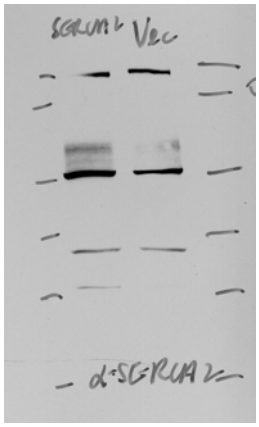

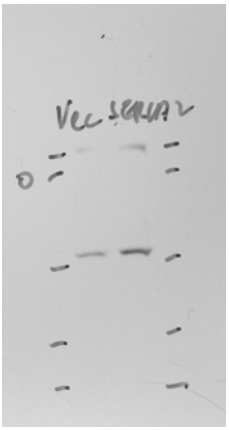

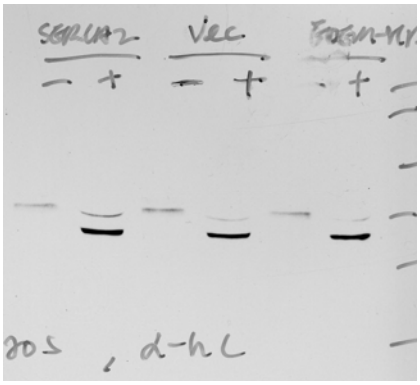

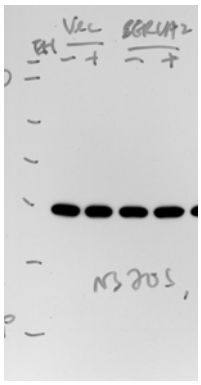

Figure 4

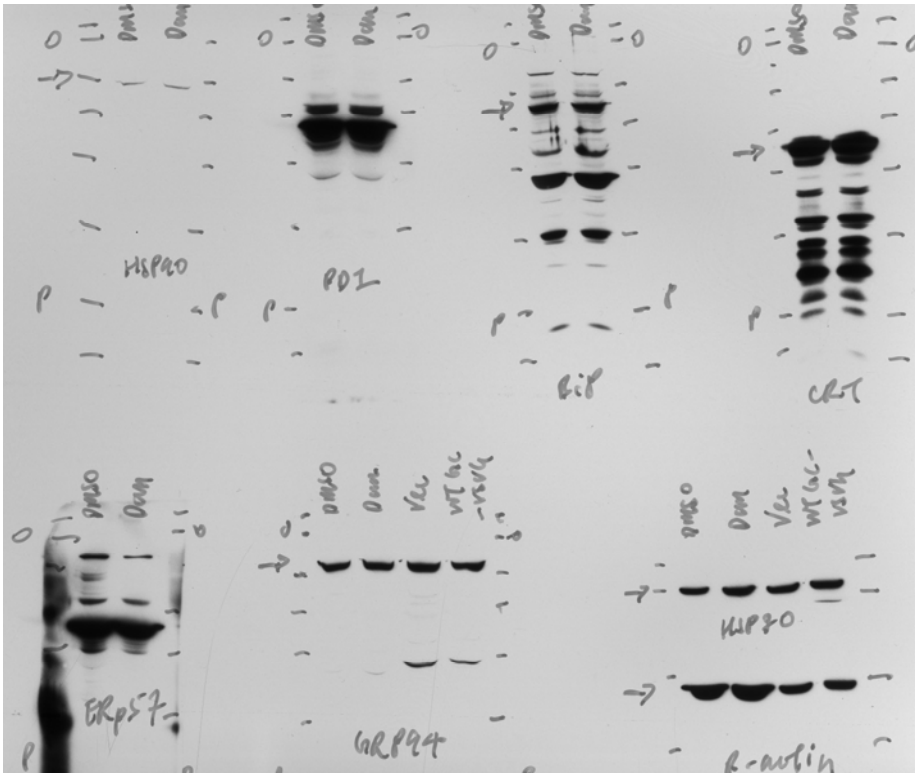

Figure 5

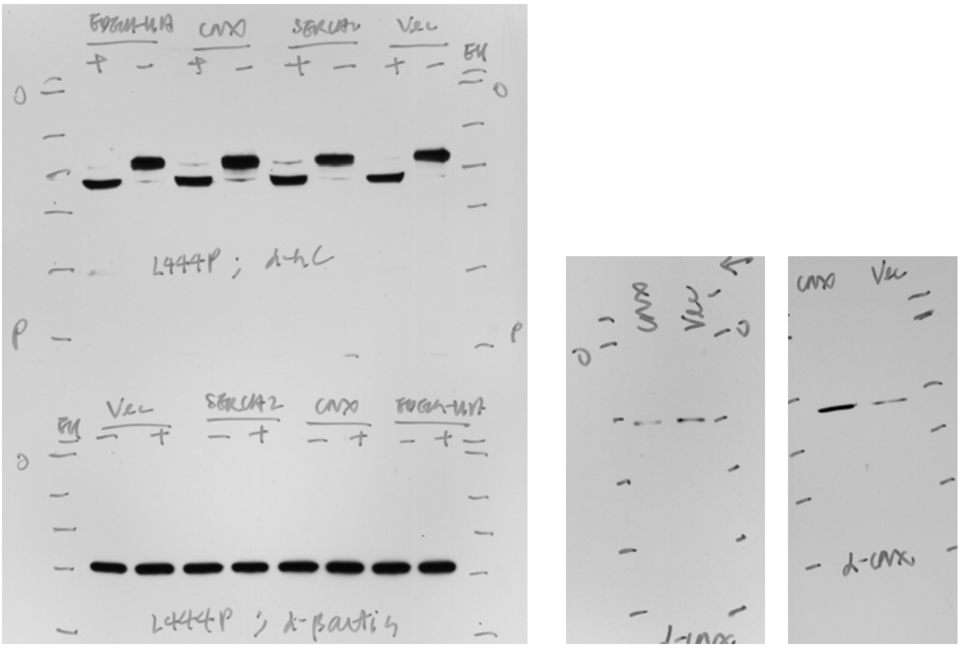

Figure 6

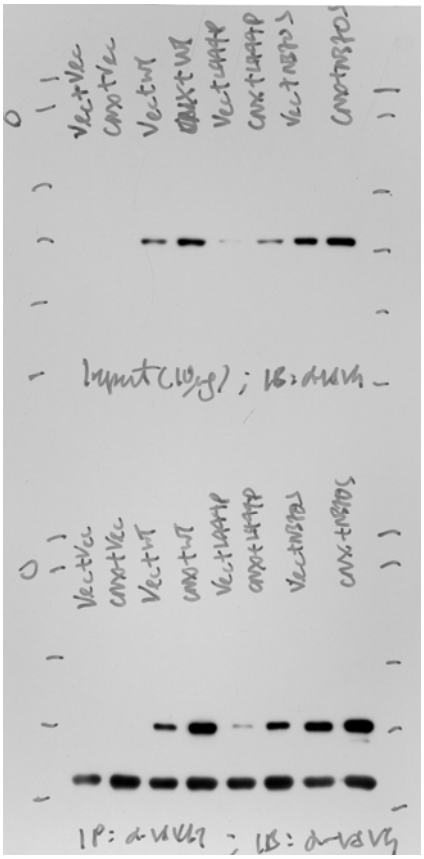

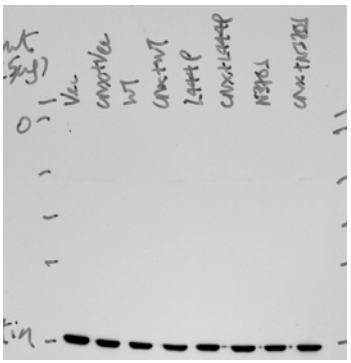

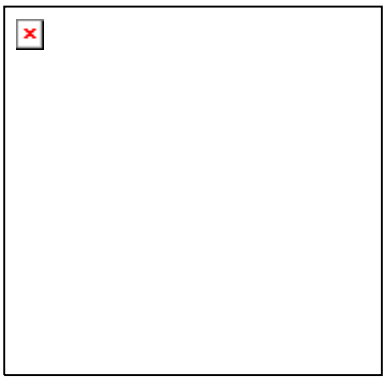

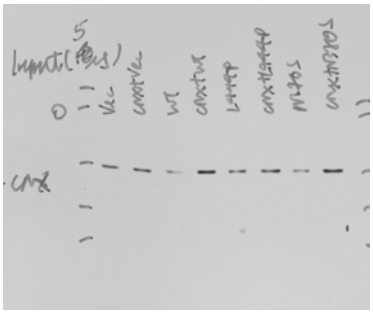

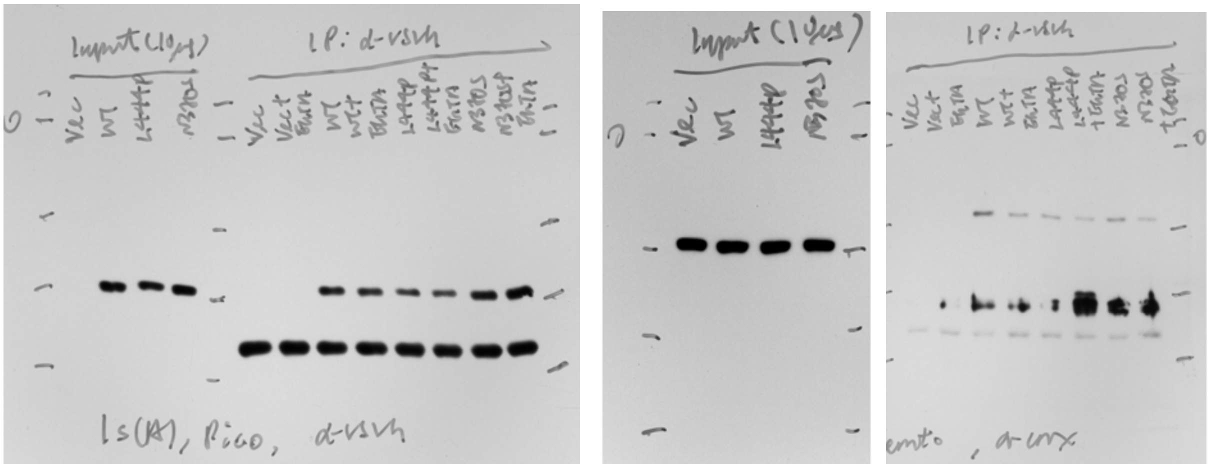
Input
IP: α-VSVh
Input
IP: α-VSVh

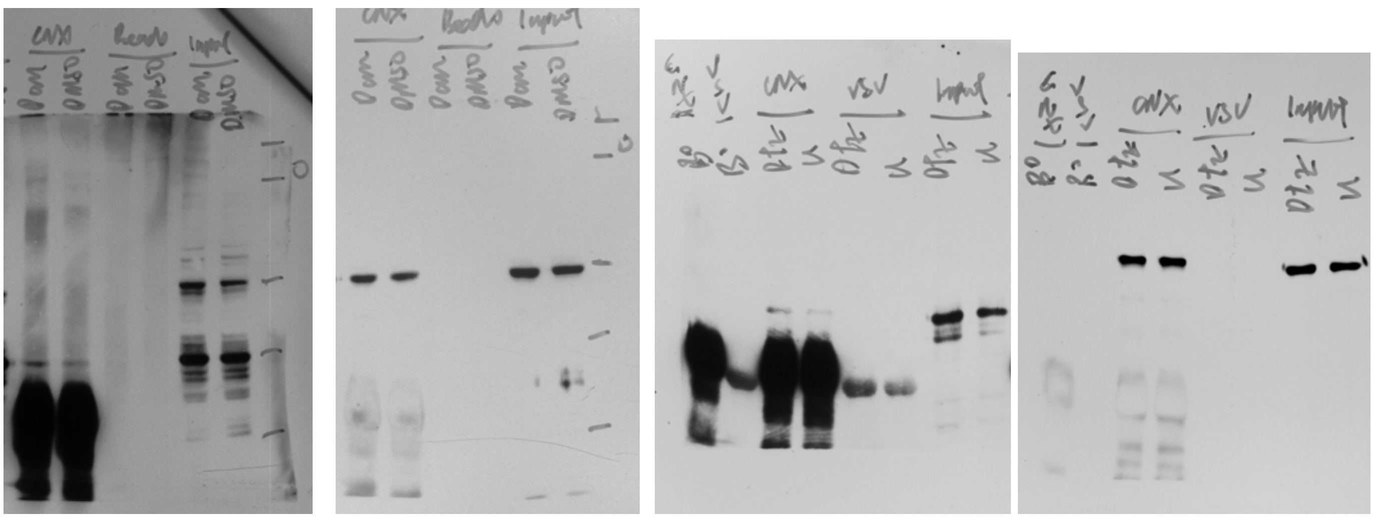
CNX
Beads
Input
CNX
Beads
Input
CNX
VSV
Input
CNX
VSV
Input

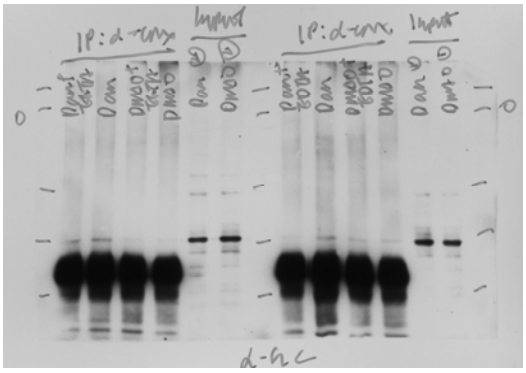

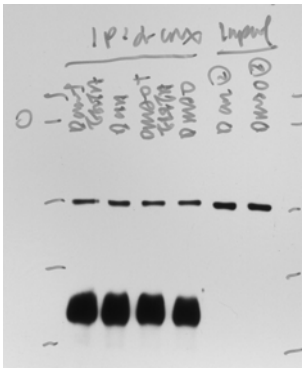

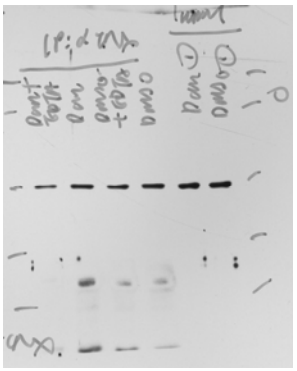

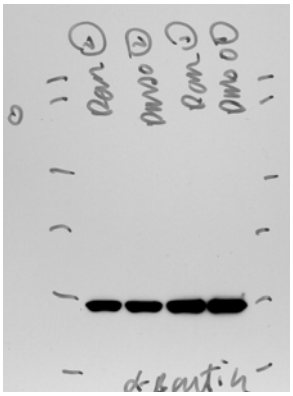

Supplementary Figure 2

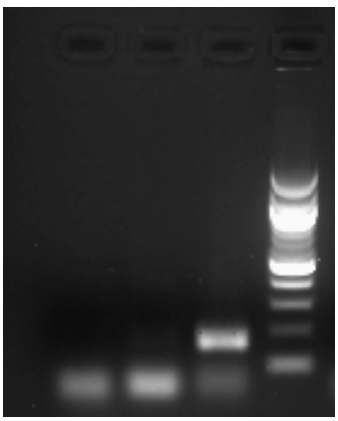

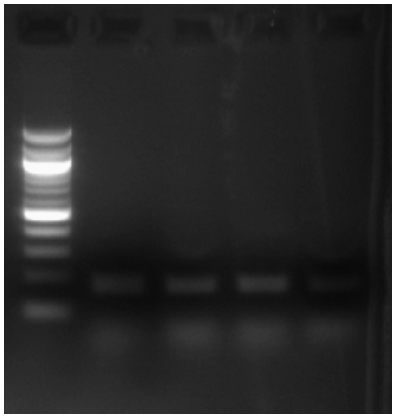

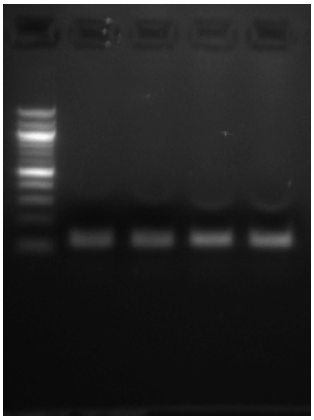

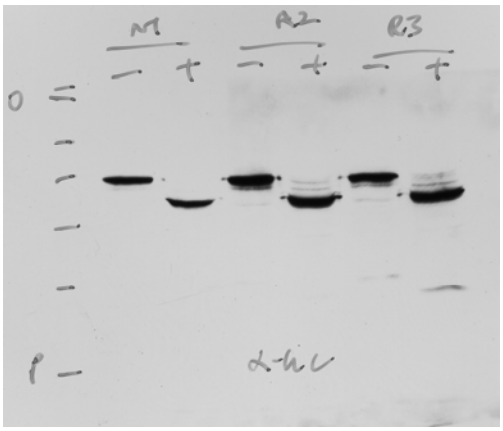

Supplementary Figure 7

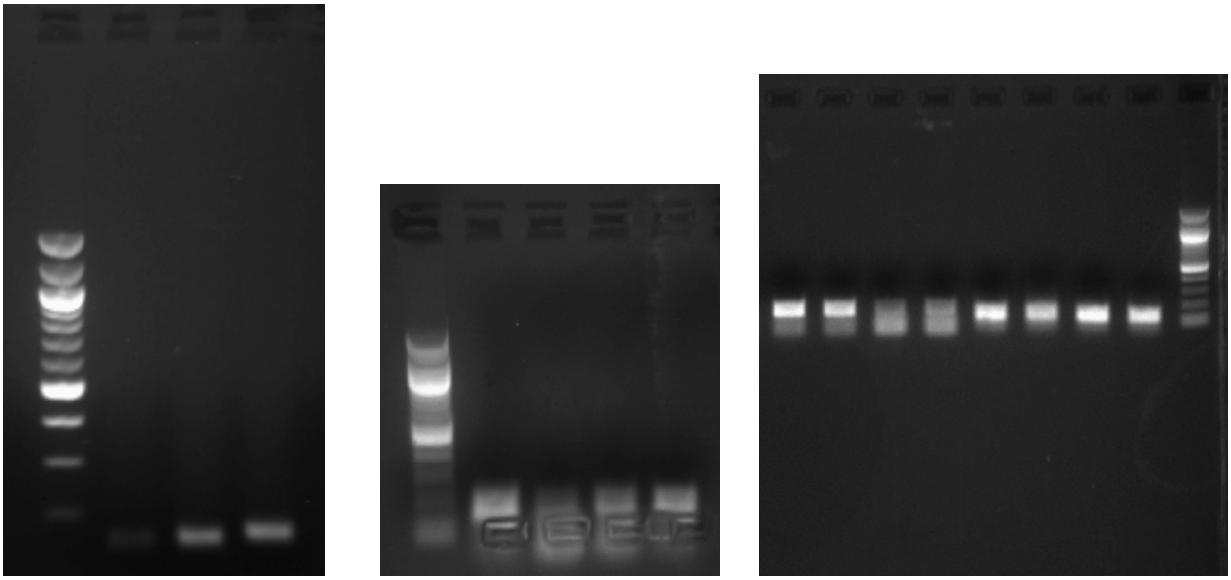

Supplementary Figure 8

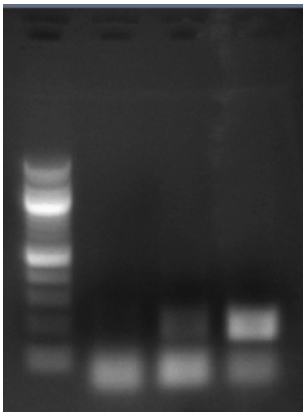

Supplementary Figure 10

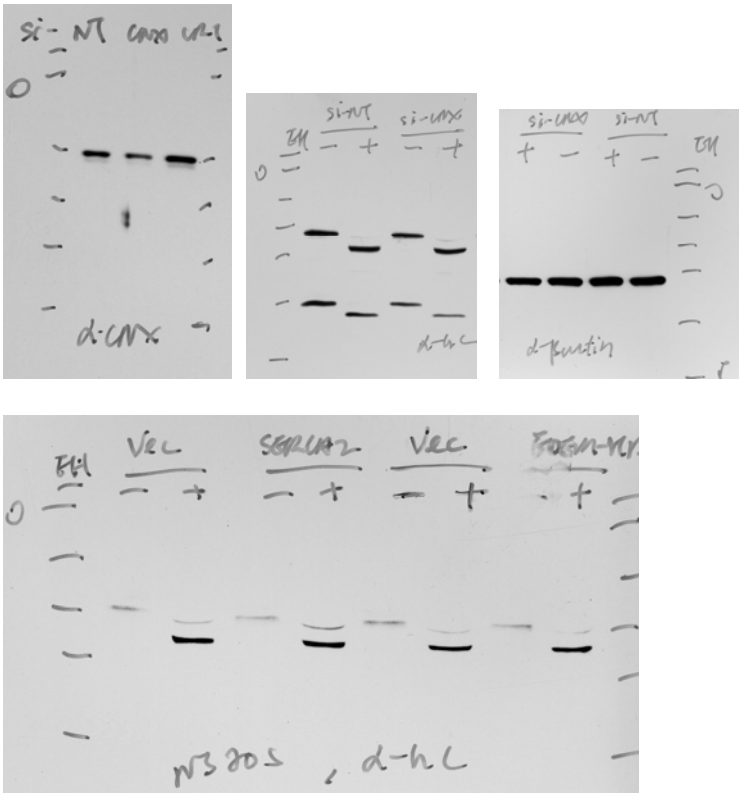

Supplementary Figure 11

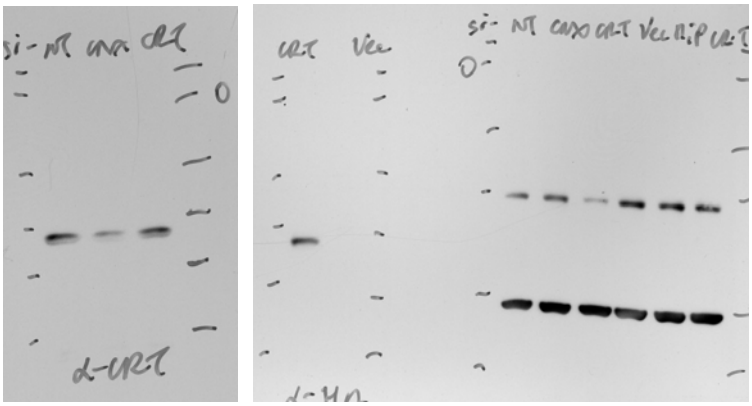

Supplementary Figure 12

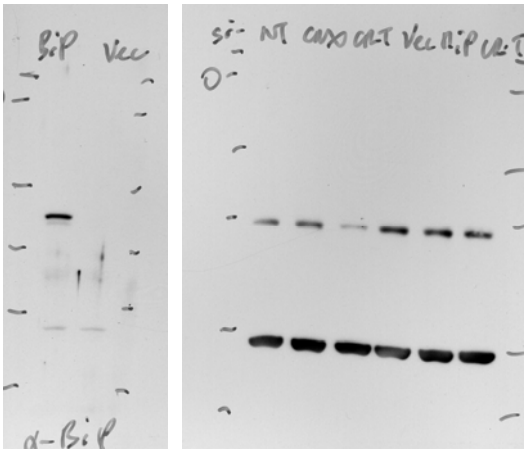

Supplementary Figure 13